Computational fluid dynamics (CFD) study on the fetal aortic coarctation

Yue Zhou[1,a], Yutao Zhang[1, b], Jingying Wang[2, c]

[1]School of Aeronautic Science and Engineering, Beihang University

Beijing, 100191, China

[2]School of Energy and Power Engineering, Shandong University

Jinan, 250061, China

*Corresponding author

[a]E-mail: yuezhou@buaa.edu.cn [b]E-mail: mileshunter13@gmail.com [c]E-mail: wjy_sdu@126.com

Abstract. Blood flows in normal and coarctate fetal aortas are simulated by the CFD technique using T-rex grids. The three-dimensional (3-D) digital model of the fetal arota is reconstructed by the computer-aided design (CAD) software based on two-dimensional (2-D) ultrasono tomographic images. Simulation results displays the development and enhancement of the secondary flow structure in the coarctate fetal arota. As the diameter narrow ratio rises greater than 45%, the pressure and wall shear stress (WSS) of the aorta arch increase exponentially, which is consistent with the conventional clinical concept. The present study also demonstrates that CFD is a very promising assistant technique to investigate human cardiovascular diseases.

1. Introduction

The cardiovascular disease is very common worldwide. Particularly, the coarctation of the aorta (CoA) has made up 5%-8% of congenital heart diseases [1], which can lead to the infantile cardiovascular failure and adult asymptomatic hypertension [1]. CoA in clinical mainly includes the arch dysplasia and isthmus dysplasia. As shown in Fig.1(a), the fetal aorta is made up of an ascending aorta (AAO), an aortic arch (AA), and a descending aorta (DAO). There are three branches on the top of AA, namely, the innominate artery (INA), the left common cartied artery (LCCA), and the left subclavian aretery (LSCA). The constriction part of the aorta between LSCA and the ductus arteriosus (DA) is called the aortic isthmus (AI). Clinically, the definition of the arch dysplasia is that the proximal diameter of the aortic arch is less than 60% of the AAO diameter and the distal diameter is less than 50% of the AAO diameter, while the the definition of the isthmus dysplasia is that the isthmus diameter is less than 40% of the AAO diameter [2].

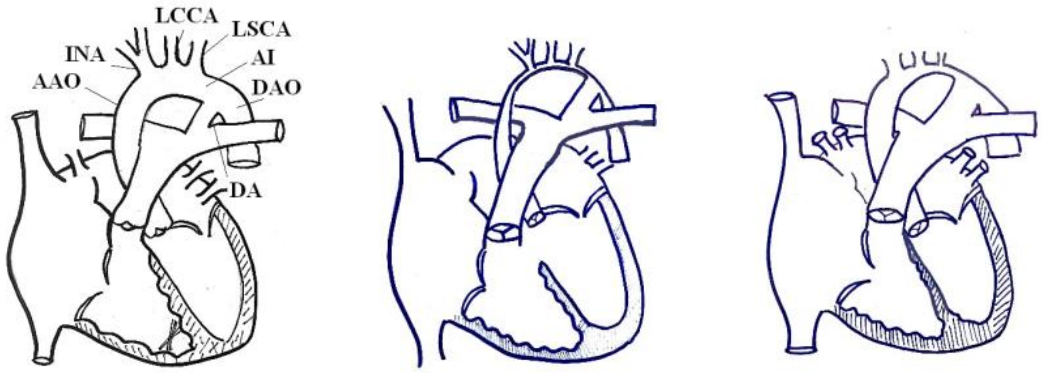

(a) (b) (c)

Figure 1: The schematic of the aorta: (a) normal; (b) arch dysplasia; (c) isthmus dysplasia.

Rencent years, CFD has been widely used to study various flow problems including the blood circulation in the human body [3], which can provide more detailed information than clinical observations, such as blood flow structures, the pressure and WSS distributions. This work employs the CFD technique to investigate the fetal aorta coarctation disease. Normal and coarctate aorta models are both reconstructed in the CAD software based on clinical ultrasouno tomographic images. Then, the simulation region in the aorta model is discretized by T-rex grids, and the blood flow is solved in the CFD software Fluent. Finally, results of blood flow structures, the pressure and WSS distributions are emphatically analyzed.

2. Methodology

2.1 Assumptions

Some assumptions are necessary before applying the CFD method to solve hemodynamic problems. When the blood is regarded as a continuum fluid medium, its viscosity mainly depends on the number of red blood cells (RBCs) in it. The more RBCs are, the greater the blood viscosity is. Although blood flows in arteries have indicated non-Newtonian effects in static or under low shear rate conditions, it can also be treated as the Newtonian fluid in the present research [4].

Another problem is that the blood flow speed varies in the aorta during a cardiac cycle period. This phenomenon makes the elastic vessel shrink and expand to some extent, which results in 5%-10% variation of the aorta diameter. Nevertheless, for simplicity, the fluid-solid interaction is not considered in the current preliminary simulation [5]. Additionally, because the turbulent flow state only happens in a short time of the whole cardiac cycle and corresponding Reynolds and Womersley numbers are both small, the blood flow in the fetal aorta is assumed to be steady and laminar in this work [6].

2.2 Governing Equations

According to assumptions in Sec.2.1, the aortic blood flow is supposed to be the incompressible laminar flow. At the same time, effects of the energy transfer, gravity and body posture are all ignored. Therefore, the continuity equation describing the mass conservation of the blood flow in the aorta with joint branches is expressed as follows:

$$\nabla \cdot \boldsymbol{U} = 0 \tag{2.1}$$

where $\boldsymbol{U} = (u, v, w)^{\mathrm{T}}$ is the blood flow velocity vector. Based on the conservation law of the momentum, the blood flow obeys the Navier-Stokes (N-S) equation as

$$\frac{\partial \rho \boldsymbol{U}}{\partial t} + \nabla \cdot \left(\rho \boldsymbol{U}\boldsymbol{U} \right) = -\nabla p + \nabla \cdot \boldsymbol{\tau} + \rho \boldsymbol{f} \tag{2.2}$$

where ρ is the blood density set to be 1057 kg/m^3. With the help of the continuity equation (2.1), the momentum equation (2.2) can be rewritten as:

$$\rho\left[\frac{\partial \boldsymbol{U}}{\partial t}+\left(\boldsymbol{U}\cdot\nabla\right)\boldsymbol{U}\right]=-\nabla p+\nabla\cdot\boldsymbol{\tau}+\rho\boldsymbol{f} \tag{2.3}$$

where $\boldsymbol{f}$ is the body force and $\boldsymbol{\tau}$ is the shear stress tensor. Implementing the Newtonian fluid assumption, the shear stress tensor can be calculated by

$$\boldsymbol{\tau}=\mu\left[\nabla\boldsymbol{U}+\left(\nabla\boldsymbol{U}\right)^{T}\right] \tag{2.4}$$

where μ is the dynamic viscosity of the blood. For the fetus blood, there is μ = 0.0087kg/(m·s). Therefore, the incompressible viscous N-S equation of the aortic blood flow is

$$\rho\left[\frac{\partial \boldsymbol{U}}{\partial t}+\left(\boldsymbol{U}\cdot\nabla\right)\boldsymbol{U}\right]=-\nabla p+\nabla\cdot\mu\left[\nabla\boldsymbol{U}+\left(\nabla\boldsymbol{U}\right)^{T}\right]+\rho\boldsymbol{f} \tag{2.5}$$

The CFD technique obtains blood flow results by solving above Eq.(2.5).

3. CAD model reconstruction

2-D ultrasono tomographic images of the fetal aorta are scanned and exported layer-by-layer with an interval of 0.5mm from bottom to top of the fetus body. Then, a centerline is set and fixed to the middle of the aorta, and the outline of the aorta at each image layer is extracted by recognizing the gray feature. Therefore, a series of geometric data of the fetal aorta at each parallel scanning cross-section can be given [7].

In a CAD software, uniformly spaced parallel planes are first created equivalent to the ultrasonic scanning cross-sections. Next, the previous cross-section outline data of the aorta vessel is input on each CAD plane one by one. Then, 3-D fetal aorta model as shown in Fig.2(a) is reconstructed through a high-precision 3-D lofting method.

The concerned regions in this work mainly include the aortic arch with joint branches and portion of DA. The part of DA close to the pulmonary artery is ignored, which has little influence on the blood flow of interest. Therefore, DA segment serves as a blood flow inlet in this research. The key geometric parameters of the normal fetal aorta are set as follows:

1) The diameter of the AAO inlet is 4.2mm;
2) The diameter of the middle cross-section between INA and LCCA is 4.1mm;
3) The diameter of the middle cross-section between LCCA and LSCA is 3.8mm;
4) The AI diameter is 2.7 mm;
5) The diameter of the DAO outlet is 4.8mm;
6) The major axis diameter and minor axis diameter of the DA inlet are 4.0mm and 3.2mm, respectively;
7) the diameter of INA is 2.8mm;
8) the diameter of LCCA is 2.5mm;
9) the diameter of LSCA is 2.2mm.

On the basis of the 3-D digital model of the normal aorta, several control cross-sections are inserted in order to conveniently generate diseased models. Then, coarctate models can be easily given only by changing corresponding geometric parameters of control cross-sections of the normal model. Additionally, simulation results are also emphatically analyzed on these control corss-sections in the next.

4. Simulation settings

T-rex grids as illustrated in Fig.2(b) are used to divide the simulation region of the fetal aorta model. T-rex is a very good grid generation technique that is suitable for viscous blood flows in the aorta and can provide high-fidelity solutions. In the current research, the number of computational grids of normal and diseased aorta models are all around 23,4000.

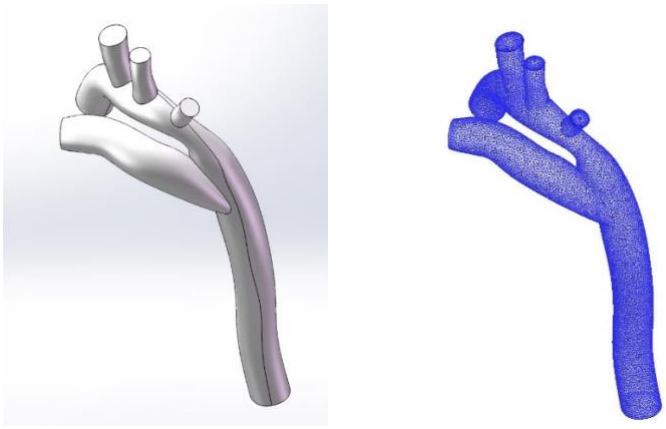

(a) (b)

Figure 2: Normal fetal aorta model: (a) geometry; (b) computational grids.

In the Fluent solver, the blood flow velocity at the AAO inlet is set to be 0.85m/s, and that of the DA inlet is 1.09m/s. According to the clinical data, the flow rate ratio is taken as 0.20 at the INA outlet, 0.12 at the LCCA outlet, 0.088 at the LSCA outlet and 0.592 at the DAO outlet.

5. Results and analysis

5.1Flowfield

The blood flow structure can be clearly displayed by the streamline mapping. Particularly, there will form the secondary blood flow in the curved aorta arch. For the more intuitive comparison, several control cross-sections, as shown in Fig.3, are selected to illustrate the blood flow structure.

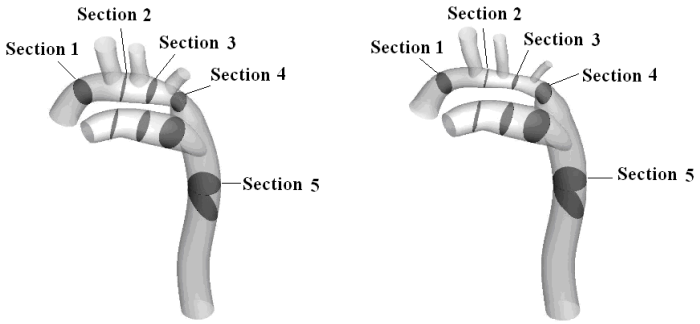

(a) (b)

Figure 3: Schematic of cross-sections: (a) normal; (b) arch dysplasia.

Figure 4 compares the streamline mappings of normal and arch dysplasia cases at each cross-section, in which the left belongs to the normal aorta and the right belongs to the arch dysplasia. At the beginning, as shown in Section 1 and 2, there is the standard secondary blood flow with the double helix structure both in the normal and dysplasia arch. As passing through joint branches, the blood flow rate gradually decreases. At the downstream of AI, the blood flow rate only remains 10% of that entering the AAO inlet, and the double helix structure becomes the single helix (Section 3 and 4). When the blood flows into the arch from the DA inlet, it can even form the triple helix structure in the diseased arch (Section 5). The blood velocity through the dysplasia arch is much greater than that in the normal aorta, as list in Tab.1. However, compared to the normal aorta, the secondary blood flow structure has no remarkable variation in the isthmus coarctation case.

Table 1: The mean blood flow velocity at each cross-section (unit: m/s).

Section No.	Normal	Coarctate

1	1.210	1.826
2	1.182	2.142
3	0.947	2.289
4	0.721	1.580
5	1.234	1.251

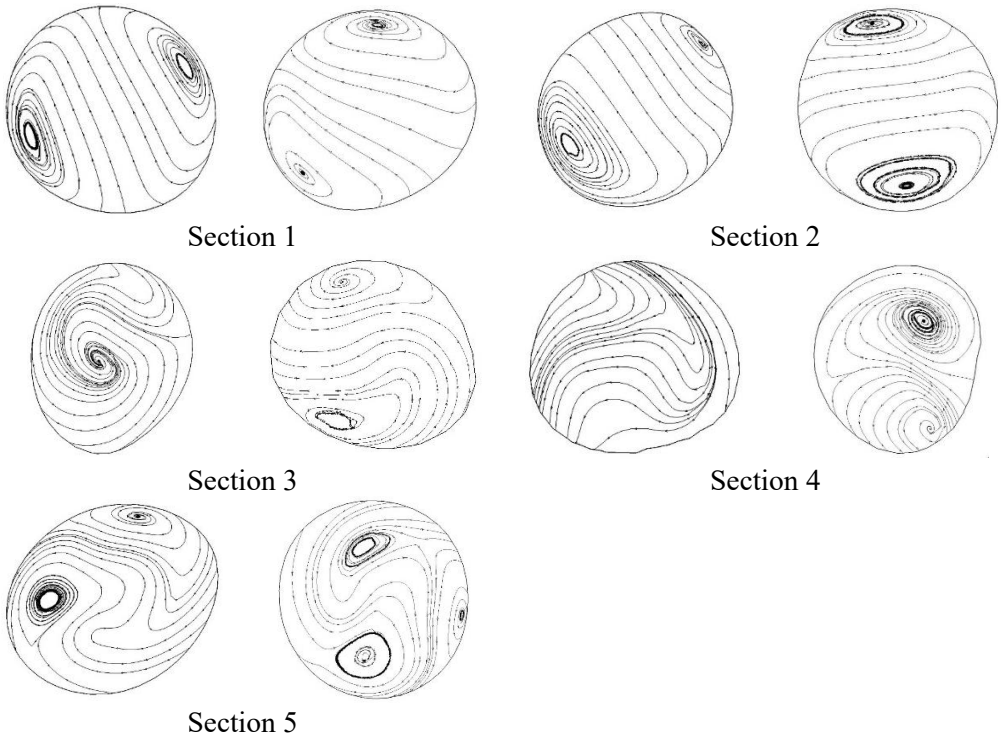

Figure 4: Streamline mapping.

5.2 Pressure and wall shear stress (WSS)

Figure 5 shows the pressure and WSS distributions of the arch dysplasia cases. From the AAO inlet to DAO outlet, the pressure gradually declines due to the wall friction, and so do in three branches. At the most region of DAO and DA, WSS keeps at a low level. Because of the large velocity gradient, WSS appears much greater at joint regions between the aortic arch and three branches than at other parts.

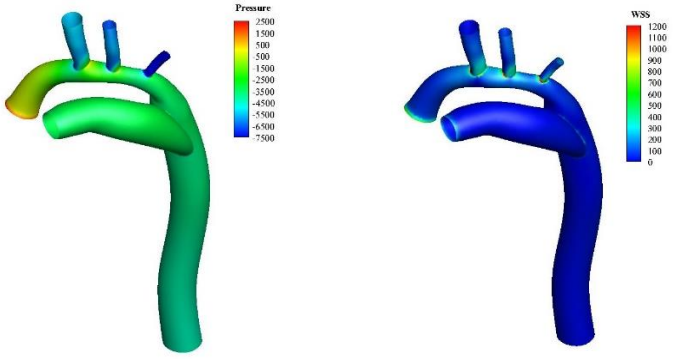

Figure 5: Results of the arch dysplasia (unit: Pa): (a) pressure; (b) WSS.

For the aortic arch dysplasia, the narrow ratio is defined as follows:

$$\text{the narrow ratio} = \frac{D_{normal} - D_{coarctation}}{D_{AAO}} \times 100\% \quad (5.1)$$

where D_{normal} is the normal diameter of the control cross-section between LCCA and LSCA, $D_{coarctation}$ is the corresponding diameter of the diseased case, and D_{AAO} is the diameter of the AAO inlet. Cases with the narrow ratio 20%, 35%, 50% and 60% are simulated respectively. Outside and inside pressure and WSS of selected control cross-sections same as in Sec.5.1 are plotted in Fig.6. When the narrow ratio is less than 20%, both the pressure and WSS vary slightly. When the narrow ratio is greater than 45%, the pressure and WSS both decrease or increase dramatically with the remarkable increase of the blood flow velocity behind the coarctation. The contraction cross-section area can accelerate the blood flow to enhance the pressure drop and WSS. For the isthmus coarctation case, WSS at the AI region is always concerned in clinical. Figure 7 shows the WSS variation as the coarctation ratio growing from 10% to 70%. WSS also rises exponentially when the narrow ratio is greater than 45%.

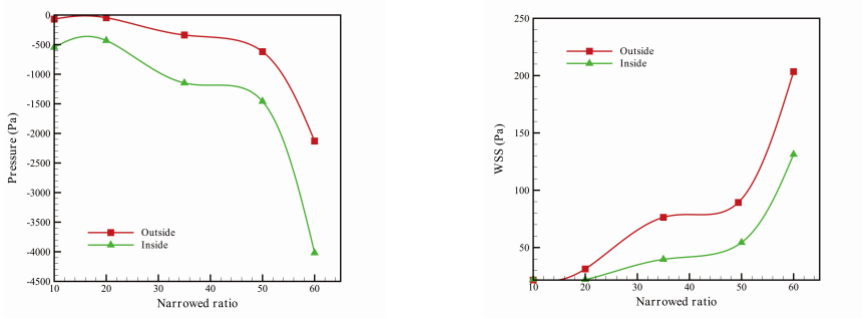

Section 1

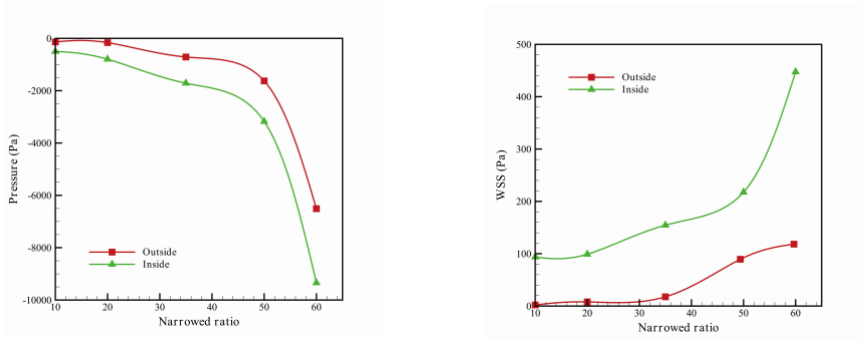

Section 2

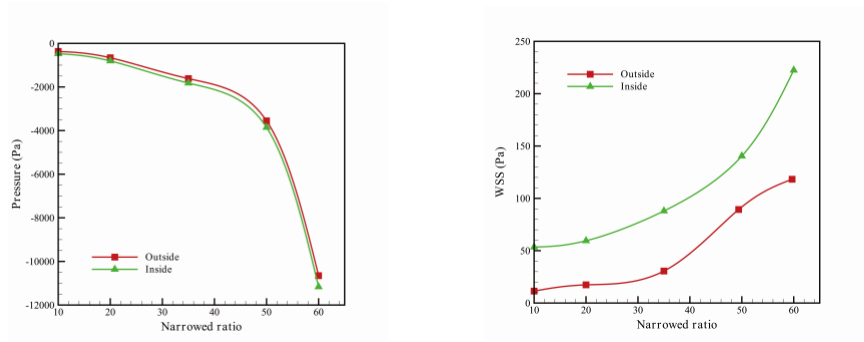

Section 3

Figure 6: Coarctation effects of the arch dysplasia.

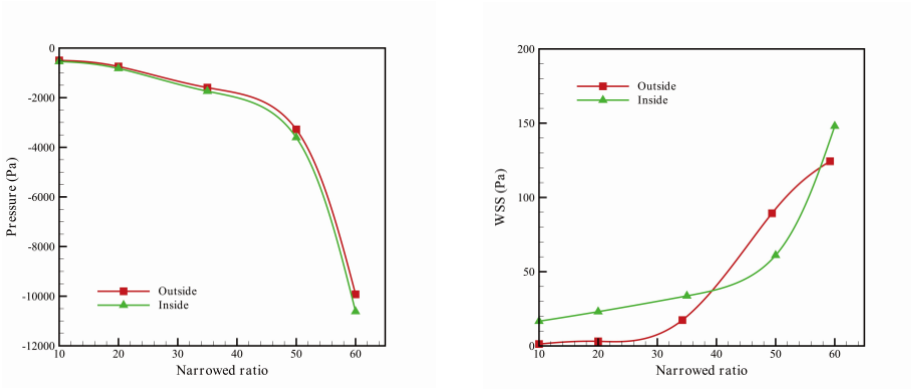

Section 4

Figure 6: Coarctation effects of the arch dysplasia. (Continued)

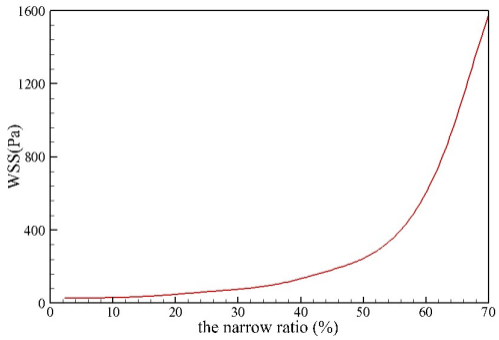

Figure 7: WSS results of the isthmus dysplasia.

6. Conclusions and discussions

In this work, 3-D digital models of the normal and coarctate fetal aorta are reconstructed based on 2-D ultrasono tomographic images, and blood flows in both normal and diseased fetal aortas are simulated by the CFD technique. Results show that, the secondary blood flow is reinforced and becomes more complex in the coarctate case compared to that in the normal aorta. The arch coarctation which reduces the cross-section area can accelerate the blood flow and increase the pressure drop and WSS remarkably.

As the narrowed ratio becomes greater than 45%, the pressure and WSS grow exponentially, which is consistent with the conventional definition in clinical. This agreement indicates that the CFD technique has the capability of reflecting the features of some cardiovascular diseases. According to the present study, it also illustrates that CFD simulation can give more details that are hardly obtained in clinical observations, such as blood flow structures, the pressure and WSS distributions. Therefore, CFD is a very promising assistant technique to investigate human cardiovascular diseases.

References

[1] M. Campbell. *Natural history of coarctation of the aorta*[J]. Heart, 1970, 32(5):633-640
[2] P. O'Brien, A. C. Marshall. *Coarctation of the aorta*[J]. Circulation, 2015, 131(9):363-365
[3] P. Gavornik, A. Dukat, L. Gaspar. *Acute and chronic aortic diseases of the thoracic and abdominal aorta of the adult - 2014 AS SMC Guidelines on the classification and diagnosis of aortic diseases*[J]. Vnitr Lek, 2015, 61(1):72-80
[4] A. Leuprecht, S. Kozerke, P. Boesiger, K. Perktold. *Blood flow in the human ascending aorta: a combined MRI and CFD study*[J]. Journal of Engineering Mathematics, 2003, 47(3):387-404

[5] F. Ghalichi, X. Deng, A. De Champlain, Y. Douville, M. King, R. Guidoin. *Low Reynolds number turbulence modeling of blood flow in arterial stenoses*[J]. Biorheology, 1998, 35(4):281-294
[6] J. Luo, J. Bai. *Research development of ultrasound Elastography*[J].China Medical Devics Information, 2005, 11(5):23-31 (In Chinese)
[7] W. W. Nichols, M. F. O'Rourke, C. Vlachopoulos. *McDonald's blood flow in arteries*[M]. Philadelphia: CRC Press, 2011: 77-109
[8] Y. He, K. Liu, L. Liu, X. Gu, Y. Zhang, J. Han, et al. *Feasibility of wholly demonstration of fetal arterial and venous system using spatio-temporal image correlation combined with high definition flow*[J]. Chinese Journal of Medical Imaging Technology, 2011, 27(9):1887-1890 (In Chinese)